Physics of the Earth and Planetary Interiors 180 (2010) 203–208

Contents lists available at ScienceDirect

Physics of the Earth and Planetary Interiors

journal homepage: www.elsevier.com/locate/pepi

Elastic anisotropy of ferromagnesian post-perovskite in Earth's D" layer

Wendy L. Mao[a,b,*], Yue Meng[c], Ho-kwang Mao[d]

[a] Geological and Environmental Sciences, Stanford University, Stanford, CA 94305, United States
[b] Photon Science, SLAC National Accelerator Laboratory, Menlo Park, CA 94025, United States
[c] HPCAT, Carnegie Institution of Washington, Argonne, IL 60439, United States
[d] Geophysical Laboratory, Carnegie Institution of Washington, Washington, DC 20015, United States

ARTICLE INFO

Article history:
Received 28 May 2009
Received in revised form 13 October 2009
Accepted 29 October 2009

Guest Editors
Kei Hirose
Thorne Lay
David Yuen

Editor
G. Helffrich

Keywords:
Post-perovskite
D" layer
Seismic anisotropy
Elasticity

ABSTRACT

We report experimental observation of a sizable elastic anisotropy in a polycrystalline sample of ferromagnesian silicate in post-perovskite (ppv) structure. Using a novel composite X-ray transparent gasket to contain and synthesize ppv in a panoramic diamond-anvil cell along with oblique X-ray diffraction geometry, we observed the anisotropic lattice strain and {1 0 0} or {1 1 0} slip-plane texture in the sample at 140 GPa. We deduced the elasticity tensor (c_{ij}), orientation-dependent compressional wave velocities, polarization-dependent shear-wave velocities, and the velocity anisotropy of the silicate ppv. Our results are consistent with calculations and indicate that with sufficient preferred orientation, the elastic anisotropy of this phase can produce large shear-wave splitting.

Earth's D" layer represents the lowermost 60–300 km of the silicate mantle lying just above the outer core. One particularly intriguing feature of this region is its seismic anisotropy, manifested in shear-wave splitting, the origin of which is an area of active, unresolved debate (*e.g.* Garnero, 2004; Helmberger et al., 2005; Lay et al., 2004). In Earth's D" layer there have been numerous observations of shear waves polarized in perpendicular directions traveling at speeds differing by approximately 0.5–1.5% which arrive as a split shear wave signal with the horizontally polarized shear wave arriving faster than the vertically polarized shear wave (*e.g.* Thomas, 2002). It has been proposed that the seismic anisotropy could be caused by an elastically anisotropic mineral which shows lattice preferred orientation (LPO) or layers or rods of materials with different elastic properties arranged in shape preferred orientation (SPO). The answer relies on knowing crucial information regarding the single-crystal elasticity and preferred crystallographic orientation of the major constituents of the D" layer which may include the post-perovskite (ppv) phase of ferromagnesian silicate (*e.g.* Mao et al., 2005, 2004; Merkel et al., 2007b; Murakami et al., 2004; Oganov and Ono, 2004; Shim, 2008; Shim et al., 2008; Tsuchiya et al., 2004b). However, due to technical difficulties, experimental examination of the single-crystal elasticity of silicate ppv has not been previously feasible, although Brillouin spectroscopy measurements on polycrystalline $MgSiO_3$ ppv have recently been reported (Murakami et al., 2007).

Elasticity information can be obtained from probing stress–strain relations in a uniaxially compressed sample. Superimposing a uniaxial compression onto a polycrystalline aggregate already under a confining pressure (P) produces a deviatoric strain (ε_ψ) that is a function of the angle (ψ) between the direction of the strain and the compression axis.

$$\varepsilon_\psi(h\,k\,l) = \frac{d_\psi(h\,k\,l) - d_P(h\,k\,l)}{d_P(h\,k\,l)} = (1 - 3\cos^2\psi)\cdot Q(h\,k\,l) \quad (1)$$

where $d_\psi(h\,k\,l)$ is the lattice spacing measured at ψ, and $d_P(h\,k\,l)$ is the lattice spacing under hydrostatic pressure. The slope $Q(h\,k\,l)$ is a constant for elastically isotropic materials, but varies with $h\,k\,l$ for elastically anisotropic materials, and may provide a quantitative measure of the direction and degree of elasticity anisotropy. Singh et al. (1998) further developed the formulism of calculating the full elastic tensor (c_{ij}'s) and velocity anisotropy based on $Q(h\,k\,l)$ and

* Corresponding author at: Geological and Environmental Sciences, Stanford University, 450 Serra Mall, Braun Bldg #320, MC 2115, Stanford, CA 94305-2115, United States. Tel.: +1 650 723 3718.
E-mail address: wmao@stanford.edu (W.L. Mao).

0031-9201/$ – see front matter © 2009 Elsevier B.V. All rights reserved.
doi:10.1016/j.pepi.2009.10.013

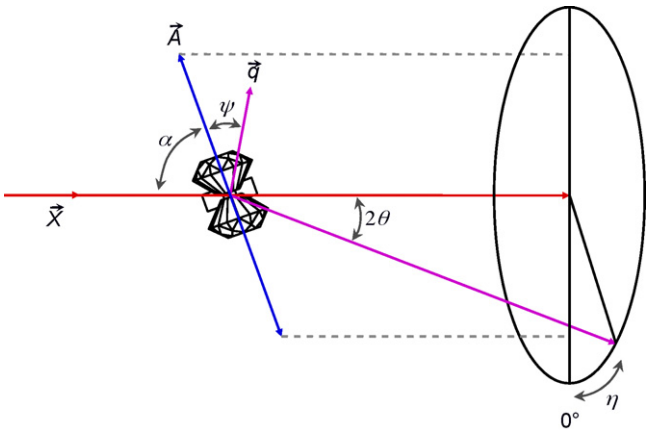

Fig. 1. Oblique X-ray diffraction geometry. 2θ is the diffraction angle; ψ is the angle between the diamond compression axis (A) and the diffraction plane normal (q); α is oblique angle between the compression axis and the X-ray beam (X); η is the azimuthal angle which is the projection of ψ on the 2D detector. They are related by: $\cos\psi = \cos\eta\cos\theta\sin\alpha - \sin\theta\cos\alpha$. After Mao et al. (2008).

additional information of axial compressibilities (χ_a, χ_b, χ_c) and aggregate shear modulus (G).

To measure strain as a function of ψ, Kinsland and Bassett (1976) developed a diamond-anvil cell that had a large side opening which could access the full range of ψ by directing X-rays perpendicular to the diamond axis (radial direction) onto the sample. Mao et al. (1998) later made modifications and developed a panoramic diamond cell which extended radial diffraction capabilities to megabar pressures by use of an X-ray transparent Be gasket, and studied the elasticity of hcp-Fe to 220 GPa with Singh formulism. This technique has also been used successfully for studying elasticity and strength of mantle silicates and oxides below 100 GPa (Kavner and Duffy, 2001; Shieh et al., 2004, 2002). One has to be careful about the orientation dependence of differential stress resulting from plastic deformation which has been shown to be potential source of error in hexagonal close-packed metals like Co (Merkel et al., 2006, 2009) and Fe at high pressure (Mao et al., 2008).

Similar study of silicate ppv using this method, however, has been fraught with experimental problems as it requires very high pressure–temperature to synthesize this phase. The sample becomes very thin at high pressure (a condition exacerbated by having to use a relatively soft, Be gasket that is further weakened by laser-heating). The low-symmetry, low intensity diffraction signal of the small silicate ppv sample, which is also a relatively weak scatterer, can be overwhelmed by diffraction from the Be gasket. These challenges have been overcome with improvements in laser-heating systems to allow for double-sided heating of the longer panoramic diamond cells, addition of a graphite insert to make a composite gasket that increases sample thickness and stability, and modifications to oblique diffraction geometry to avoid scattering of Be by the direct X-ray beam (Fig. 1).

The silicate ppv in the D" layer is likely to contain other elements like Fe (Mao et al., 2005). We chose to study a high-Fe silicate ppv with $Mg_{0.6}Fe_{0.4}SiO_3$ composition because the additional χ_a, χ_b, χ_c and G values from other sources are available for this composition for c_{ij} calculations (Mao et al., 2006). The amount of Fe is important for our ^{57}Fe nuclear resonant inelastic X-ray scattering measurements which allow use to determine G at these ultrahigh pressures. Although $Mg_{0.6}Fe_{0.4}SiO_3$ may represent an Fe-rich endmember whose composition is more relevant to ultralow-velocity zones since its absolute values of velocities significantly below that in most of the D" layer (Mao et al., 2006), its velocity anisotropy and plastic deformation characteristics can be representative of this silicate structure in general. Here we also assume that the structure for $Mg_{0.6}Fe_{0.4}SiO_3$ ppv is the same as the Mg endmember, and we found that the *Cmcm* space group fit our data reasonably well. Possible ordering of the cation sites could lead to subtle differences in the structures (e.g. multiple cation sites but same unit cell), but the spottiness of our pattern results in unreliable intensity data, so we could not differentiate between *Cmcm* and its subgroups.

For the RXD measurement, synthetic $Mg_{0.6}Fe_{0.4}SiO_3$ orthopyroxene starting material was loaded along with a small piece of Pt added for pressure calibration (Jamieson et al., 1982) into the graphite-Be composite gasket in a panoramic diamond-anvil cell. At low pressure, the soft graphite insert deforms readily and seals the sample chamber, while at increasing pressures beyond 15 GPa, graphite becomes transparent (Utsumi and Yagi, 1991), superhard, and a very weak X-ray scatterer (Mao et al., 2003) which reduces contamination of the silicate ppv X-ray pattern. The exceptional strength of high-pressure graphite maintains the sample configuration and thickness. The transparent, high-pressure graphite gasket adjacent to the heated sample does not absorb the laser and stays cool, and as a result, the sample configuration remains very stable to the maximum pressures and temperatures. Avoiding heating of the gasket also minimizes possible gasket-sample reaction.

The RXD experiment was conducted at beamline 16-IDB of the Advanced Photon Source (APS), Argonne National Laboratory (ANL). The sample was first compressed to 140 GPa and then heated with a double-sided YLF laser system operating in TEM_{01} donut mode to 2000 K which resulted in conversion into a single-phase of polycrystalline silicate ppv. We then conducted angle dispersive synchrotron X-ray diffraction measurements in an oblique radial scattering geometry (Fig. 1) using a monochromatic X-ray beam with $\lambda = 0.4158$ Å. Two-dimensional diffraction images were collected during heating and after temperature quenching. The polar X-ray diffraction images recorded on a MAR image plate were transformed into a Cartesian (cake) plot of azimuthal angle (η) versus 2θ diffraction angle (Fig. 2). These images indicate clear variations in the diffraction peak position and intensity as a function of η. The waviness of the ppv peak position of an individual $h\,k\,l$ reflection shows the change of its d-spacing resulted from the uniaxial compression, and reveals the maximum strain (shear strength) of the sample, while the difference in waviness of different $h\,k\,l$ is related to the elastic anisotropy. The intensity variation indicates preferred orientation in the sample and provides slip-plane information (Merkel et al., 2003, 2002; Miyagi et al., 2008; Wenk et al., 2000).

The silicate ppv sample shows preferred orientation, for example the 1 1 0 reflection is more intense near $\eta = 0^\circ$ (compression axis). The texture in our silicate ppv sample is qualitatively similar to that reported for $MgSiO_3$ ppv (Merkel et al., 2007b). We agree with the {1 0 0} or {1 1 0} slip-plane assignment. In the silicate ppv lattice, the b-axis is 3.3 times longer than the a-axis, and the angle between (1 0 0) and (1 1 0) is only 16.8°. Consequently, the textures produced by {1 0 0} and {1 1 0} slip-planes are very similar. Our observation is also consistent with the pathway dependent slip-plane mechanism which predicts [1 1 0] vertical alignment for a $MgSiO_3$ ppv layer (Oganov et al., 2005), instead of the earlier assumption of a {0 1 0} slip plane which is the direction of the layers (Iitaka et al., 2004; Oganov and Ono, 2004; Tsuchiya et al., 2004a), but we may be observing a transformation texture rather than a deformation texture as we did not further deform the sample and observe changes in the texture (Walte et al., 2009).

We determined the d-spacing of each $h\,k\,l$ as a function of ψ, and the lattice strain for different $h\,k\,l$ reflections as shown in Fig. 3. To solve for the elastic compliance tensor elements (s_{ij}), the following relation from Singh formulism was used for the orthorhombic